

# MEMS MIDDLE EAR ACOUSTIC SENSOR FOR A FULLY IMPLANTABLE COCHLEAR PROSTHESIS

*M. A. Zurcher<sup>1</sup>, D. J. Young<sup>1</sup>, M. Semaan<sup>2</sup>, C. A. Megerian<sup>2</sup>, and W. H. Ko<sup>1</sup>*

<sup>1</sup>Department of Electrical Engineering, Case Western Reserve University, Cleveland, Ohio, USA

<sup>2</sup>Department of Otolaryngology, University Hospitals of Cleveland, Cleveland, Ohio, USA

## ABSTRACT

A MEMS accelerometer is proposed as an implantable middle ear microphone for a future fully implantable cochlear prosthesis. Vibration characterization of human temporal bones indicates that a MEMS accelerometer needs to achieve a sensing resolution of  $75 \mu\text{g}_{\text{rms}}/\sqrt{\text{Hz}}$  with a bandwidth of 10 kHz to detect normal conversation. A prototype MEMS accelerometer is designed and fabricated. The device exhibits a nominal capacitance value of 2.4 pF with a differential sensitivity of 4 fF/g. When interfaced with a low noise CMOS capacitance-to-voltage converter, the sensor achieves a sensing resolution of  $78 \mu\text{g}_{\text{rms}}/\sqrt{\text{Hz}}$  at 500 Hz with a sensitivity of 11.5 mV/g and bandwidth of 6.4 kHz. The overall system attached on umbo demonstrates the capability of detecting normal conversation.

## INTRODUCTION

Over 20 million people in the United States and millions more around the world are affected by sensorineural hearing loss. Contemporary acoustic hearing aids can achieve moderate rehabilitation in a large number of sensorineural hearing loss cases. However, inherent technological limitations and perceived social stigma associated with these devices have resulted in many patients being deprived of basic hearing abilities. While partially implantable middle ear and cochlear prosthetic systems have become increasingly accepted, the use of external accessories such as microphones and electronics presents reliability, practicality, and social stigma concerns. Therefore, it is highly desirable to develop fully implantable high-performance prosthetic systems.

While progress has been made in developing and improving middle ear implantable systems that rely on piezoelectric effects [1] and electromagnetics [2] - [3] for compensation of hearing loss, these approaches do not address cochlear hair cells damage, which causes sensorineural hearing loss and is responsible for the majority of all hearing loss cases. Although modern semi-implantable cochlear implants address hair cells damage by direct stimulation of the auditory nerve, the implants continue to rely on an external microphone, speech processor, and radio frequency coils. The speech processors can be potentially integrated as a part of the existing implant unit. However, a significant challenge is presented in realizing a high-performance implantable microphone. This

paper describes a MEMS accelerometer proposed as an implantable middle ear microphone for a future fully implantable cochlear prosthesis. Figure 1 presents the proposed conceptual prosthetic system architecture.

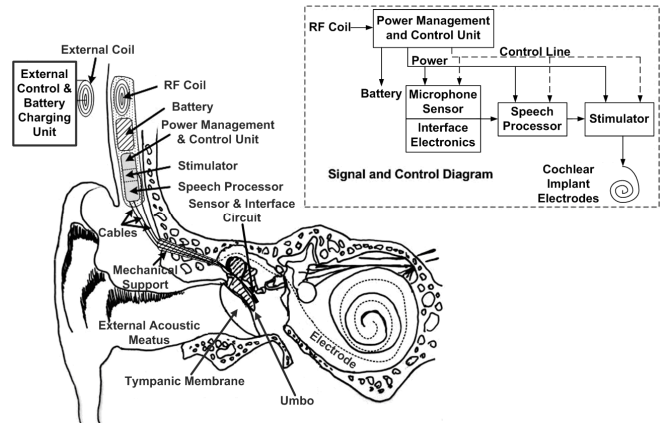


Figure 1. Proposed fully implantable cochlear prosthetic system architecture.

Based on accelerometer operating principle, the proposed middle ear microphone can be attached to the umbo to convert the bone vibration to an electrical signal representing the input acoustic information. Further processing of the electrical signal can be performed by the cochlear implant speech processor, which is followed by a stimulator to drive cochlear electrodes. The speech processor, stimulator, power management and control unit, rechargeable battery and radio-frequency (RF) coil can be housed in a biocompatible package located under the skin to form a wireless communication link with the external adaptive control and battery charging system. The proposed accelerometer-based middle ear microphone design is attractive due to its long-term stable performance, unlike the conventional microphone with its performance susceptible to degradation due to tissue encapsulation and scar formation after implant [4].

## ACCELEROMETER DESIGN

Previous research using an optical method to characterize micro-mechanical behavior of the ossicular chain in human temporal bones has determined the optimum location and orientation for the proposed accelerometer placement: on the umbo oriented to sense acceleration perpendicular to the plane of the eardrum [5]. Important low frequency vibratory characteristics of the umbo can be further

enhanced by removing the incus [6]. Optical measurements of temporal bones performed with the incus removed indicate that in order to detect normal conversation, the proposed MEMS-accelerometer-based middle ear microphone needs to achieve a sensing resolution of  $75 \mu\text{g}_{\text{rms}}/\sqrt{\text{Hz}}$  with a bandwidth of 10 kHz and a packaged mass of 20–25 milligrams.

Figure 2 presents the proposed accelerometer general architecture. The differential capacitive lateral-axis sensing topology is chosen due to its fabrication simplicity, common-mode interference rejection, and straight forward interfacing with low noise differential capacitance-to-voltage conversion circuitry.

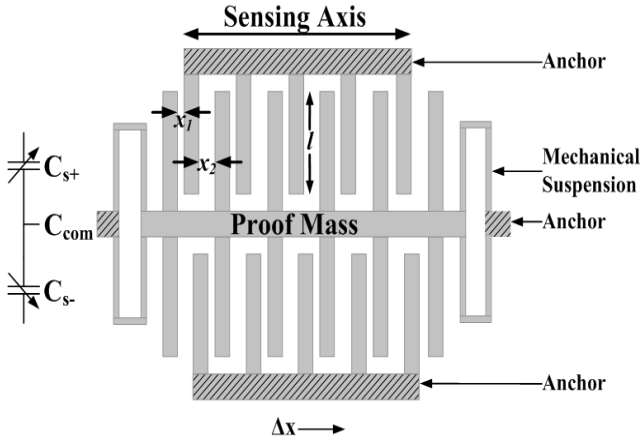


Figure 2. Prototype MEMS accelerometer architecture.

The interdigitated sensing fingers form a set of parallel sensing capacitors on both sides of the proof mass. The nominal capacitance value from each side is a function of the overlap finger length,  $l$ , device layer thickness,  $t$ , air gap between adjacent fingers,  $x_1$  and  $x_2$ , and the number of sensing finger sets  $N$ , according to equation (1).

$$C_{s+nom} = \left( \frac{\epsilon_0 l t}{x_1} + \frac{\epsilon_0 l t}{x_2} \right) \times N = C_{s+1} + C_{s+2} \quad (1)$$

The shuttle moves along the direction of acceleration and thus changes the gap spacing between the interdigitated fingers by  $\Delta x$ , which results in a corresponding change in sensing capacitance value as expressed in equation (2).

$$\Delta C_{s+} = \left( \frac{\epsilon_0 l t}{x_1} \frac{\Delta x}{x_1} - \frac{\epsilon_0 l t}{x_2} \frac{\Delta x}{x_2} \right) \times N \quad (2)$$

If the gap spacing of  $x_1$  and  $x_2$  is identical, then there will be no capacitance change. By extending  $x_2$  much larger than  $x_1$  the second term in equation (2) can be greatly minimized, thus enhancing the sensitivity if  $N$  is unchanged. However, enlarging  $x_2$  would reduce the number of fingers that can be fabricated within a given length, thus degrading sensitivity. Analysis shows that an optimal design can be obtained if  $x_1$  is chosen to be  $2 \mu\text{m}$ , which is the minimum feature size of the fabrication technology, and  $x_2$  is chosen to be  $8 \mu\text{m}$  for a fixed device length.

The acceleration sensing resolution limited by the Brownian noise is a critical design consideration for the

MEMS accelerometer. The acceleration noise floor is proportional to the device mechanical resonant frequency and inversely proportional to the proof mass and mechanical quality factor ( $Q$ ) [7]. For a sensor bandwidth of 10 kHz and an estimated  $Q$  of unity in ambient, a proof mass of 2.5 micrograms is required to achieve a sensing resolution of  $75 \mu\text{g}_{\text{rms}}/\sqrt{\text{Hz}}$  at room temperature. The prototype accelerometer is designed with 189 sets of sensing fingers on each side of the proof mass. The fingers exhibit a thickness, width, and overlap dimension of  $25 \mu\text{m}$ ,  $2 \mu\text{m}$ , and  $96 \mu\text{m}$ , respectively, thus achieving a nominal capacitance of 2 pF. The sensor is laid out in an area of 1 mm x 1 mm with an estimated proof mass of 14 micrograms, which is well above the requirement to ensure a low noise performance. The proof mass is suspended by mechanical springs with a total compliance of 54 N/m, corresponding to a mechanical resonance of 10 kHz and differential sensitivity of 5 fF/g. With an assumed  $Q$  of unity in ambient, the sensor is expected to exhibit a Brownian noise floor of  $30 \mu\text{g}_{\text{rms}}/\sqrt{\text{Hz}}$ .

To satisfy the overall system sensing resolution requirement, the accelerometer needs to be interfaced with a low noise capacitance-to-voltage conversion circuitry as shown in Figure 3. The MEMS accelerometer, modeled as differential capacitors, is driven by a stimulation clock with an amplitude,  $V_s$ , of 1.2V and is interfaced by a differential charge amplifier, which converts the sensor capacitance change to an output voltage [8].

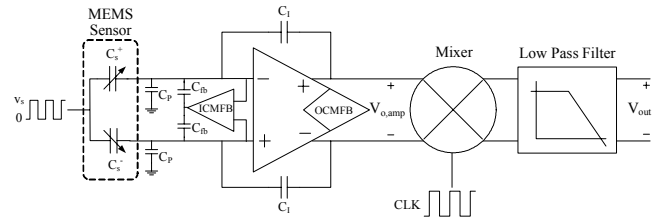


Figure 3. Sensor electronic interfacing architecture.

A clock frequency of 675 kHz is used to modulate the sensor information away from the  $1/f$  noise of the amplifier, critical for achieving a high sensitivity. An input common-mode feedback (ICMFB) circuit is designed to suppress any output offset due to the parasitic capacitance mismatch and drift over time. The charge amplifier output is then mixed by the same clock and low-pass filtered to obtain the desired analog acceleration information. With a low noise charge amplifier exhibiting an input referred noise floor of  $5 \text{nV}_{\text{rms}}/\sqrt{\text{Hz}}$ , an acceleration sensing resolution of  $25 \mu\text{g}_{\text{rms}}/\sqrt{\text{Hz}}$  is expected.

## PROTOTYPE CHARACTERIZATION

The accelerometer is fabricated by a commercial SOI MEMS process. Figure 4 presents an SEM of the fabricated sensor, which exhibits a measured nominal capacitance value of 2.4 pF.

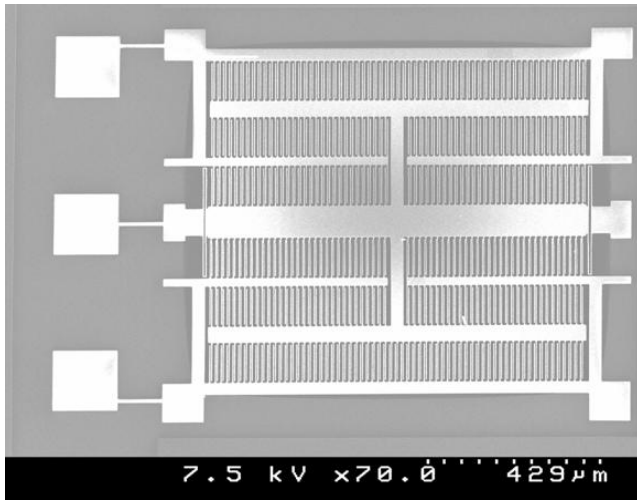


Figure 4. SEM of prototype accelerometer.

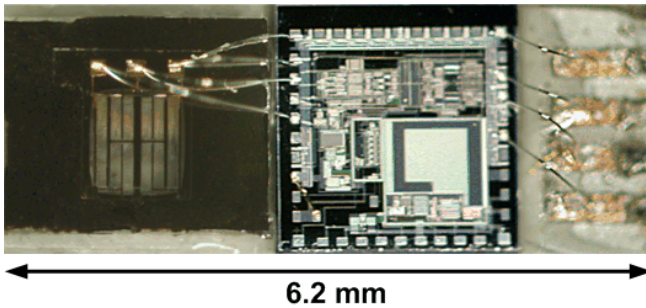


Figure 5. Hybrid middle ear implantable microphone consisting of MEMS accelerometer and interface electronics packaged on a flexible substrate.

The accelerometer is wire bonded to a custom-designed CMOS capacitance-to-voltage converter over a thin flexible substrate, as shown in Figure 5, excluding package cover. The overall system weights about 25 milligrams and achieves a sensitivity of 11.5mV/g (equivalent to 4.0 fF/g) and a noise floor of  $900 \text{ nV}_{\text{rms}}/\sqrt{\text{Hz}}$  in ambient at 500 Hz (equivalent to  $78 \text{ } \mu\text{g}_{\text{rms}}/\sqrt{\text{Hz}}$ ).

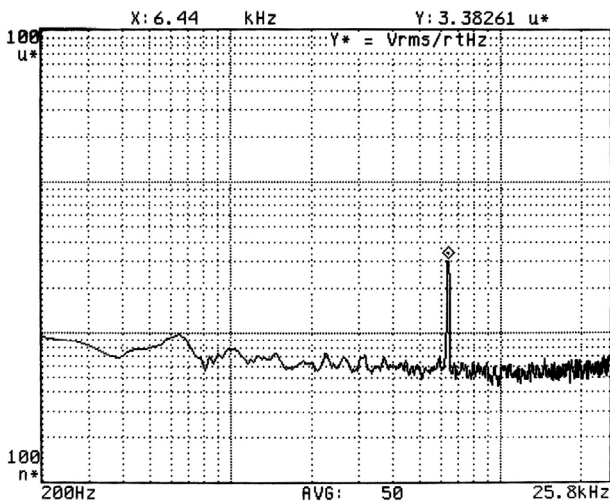


Figure 6. Output noise power spectrum in vacuum.

Figure 6 shows the measured output noise power spectral density in a 50 milli-Torr vacuum. The spectrum indicates a reduced noise floor of approximately  $800 \text{ nV}_{\text{rms}}/\sqrt{\text{Hz}}$  at 1 kHz, limited by the electronic noise, with a mechanical resonance of 6.44 kHz. The higher electronic noise floor than the designed value is due to the larger parasitic capacitance associated with the prototype system. The lateral over-etch of the microstructure reduces the suspension compliance, thus a lowered bandwidth.

## SYSTEM IMPLANT

The sensing system is then surgically attached to an umbo with the incus removed for implant performance evaluation as shown in Figure 7. Audio input stimuli with various amplitudes are applied for characterization.

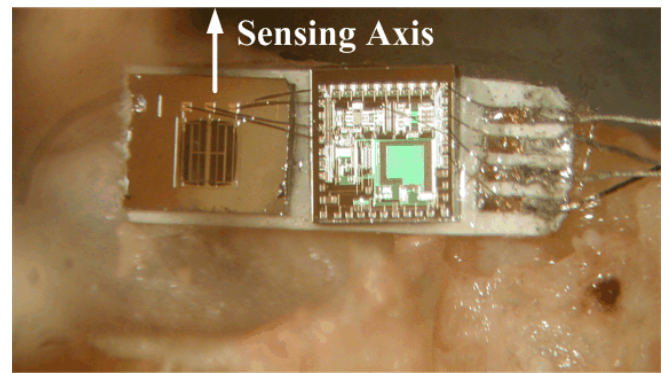


Figure 7. Prototype middle ear microphone implanted on the umbo of a human temporal bone. The arrow indicates direction of umbo movement being measured.

The accelerometer output signals in response to external sounds are recorded. The sensor is also used as a target for a laser Doppler vibrometer (LDV) to simultaneously measure acceleration optically to confirm characterization accuracy and also determine any loading effects associated with the attached mass. Figure 8 presents the acceleration frequency response of the umbo measured optically (with an input stimulus of 95 dB SPL) with and without the prototype accelerometer attached, as well as the electrical data measured with the sensor attached on the umbo.

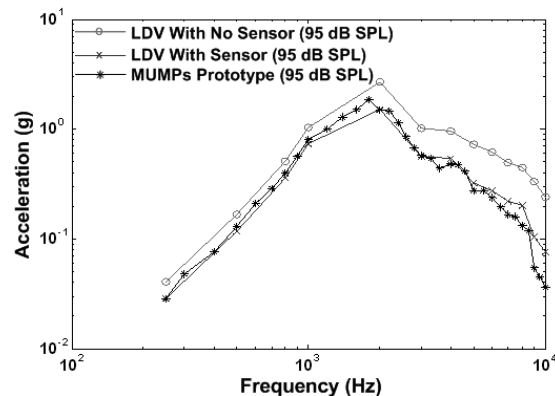


Figure 8. LDV and electrical measurements of umbo acceleration vs. frequency with and without the prototype system attached at 95 dB SPL.

The optical measurement taken with the sensor attached on the umbo shows a 3 dB suppression of acceleration below 2 kHz due to the mass loading. The signal suppression further increases to 5 dB between 2 and 8 kHz, and 10 dB above 8 kHz. This undesirable effect can be suppressed by employing an accelerometer with a further reduced packaged mass and also by implementing an alternative wiring and adhesion scheme.

Figure 9 shows the output spectrum when stimulated by a 95 dB SPL tone at 500 Hz, achieving a 40 dB SNR for a measurement bandwidth of 61 Hz. This is equivalent to a 35 dB SNR for a 200 Hz bandwidth, which is a typical bandwidth for a cochlear implant electrode focusing on 500 Hz stimulation. Therefore, the prototype microsystem is capable of sensing a 60 dB SPL tone at 500 Hz, corresponding to a detection threshold for sensing normal conversation.

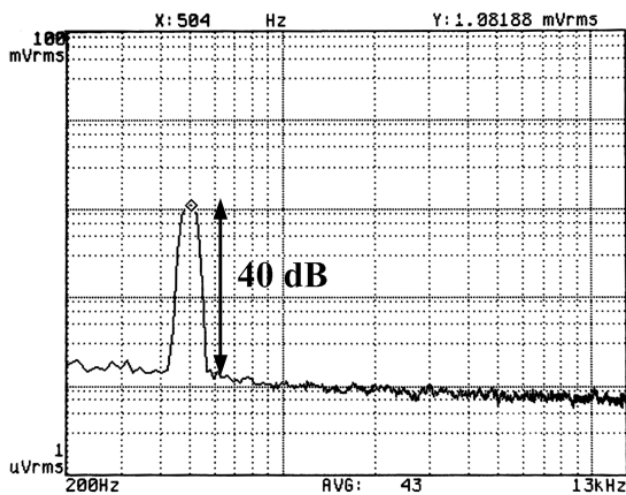


Figure 9. Accelerometer output spectrum on umbo when stimulated by 95 dB SPL at 500 Hz.

Figure 10 plots the measured sound detection threshold within a 200 Hz bandwidth over the audio spectrum, indicating that the proposed middle ear microphone is capable of detecting normal conversation.

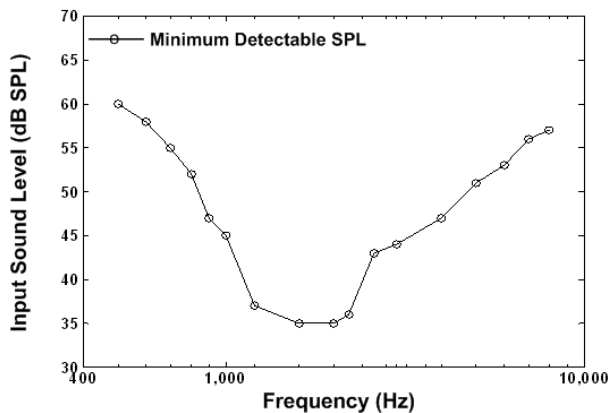


Figure 10. Minimum detectable sound level of middle ear microphone.

## CONCLUSION

A MEMS accelerometer interfaced with low noise electronics can detect and convert natural middle ear bone vibration to an electrical signal in response to normal speech. The sensor exhibits a nominal capacitance value of 2.4 pF and achieves a sensing resolution of  $78 \mu\text{g}_{\text{rms}}/\sqrt{\text{Hz}}$  at 500 Hz with a bandwidth of 6.4 kHz. The overall system attached on umbo demonstrates the capability of detecting normal conversation. Using the proposed sensor as an implantable microphone can enable the realization of a future fully implantable cochlear prosthesis.

## ACKNOWLEDGEMENT

This work was supported by the NIH (5R21-DC-006850).

## REFERENCES

- [1] H. P. Zenner, J. W. Baumann, G. Reischl, *et. al.*, "Patient selection for incus body coupling of a totally implantable middle ear implant," *Acta Otolaryngology*, vol. 123(6), pp. 683-696, August 2003.
- [2] A. Uziel, M. Mondain, P. Hagen, F. Dejean, and G. Doucet, "Rehabilitation for high frequency sensorineural hearing impairment in adults with the Symphonix Vibrant Soundbridge: A comparative study." *Otology and Neurotology*, vol. 24, pp. 775-783, 2003.
- [3] W. H. Ko, W. L. Zhu, M. Kane, and A. Maniglia, "Engineering principles applied to implantable otologic devices." *Otolaryngology Clinics of North America*, vol. 34, pp. 299-314, 2001.
- [4] H. Leysieffer, J. W. Baumann, R. Mayer, D. Müller, T. Schön, A. Volz, and H. P. Zenner, "A Totally Implantable Hearing Device for the Treatment of Sensorineural Hearing Loss: TICA LZ 3001," *HNO*, vol. 46, pp. 853-863, 1998.
- [5] M. A. Zurcher, D. J. Young, T. Trang, C. A. Megerian, W. H. Ko, "Development of Middle Ear Acoustic Sensor for Fully Implantable Cochlear Prosthesis," *the 3rd International Workshop on Network Sensing System (INSS '06)*, May 2006, pp. 49-54.
- [6] M. A. Zurcher, D. J. Young, M. Semaan, C. A. Megerian, W. H. Ko, "Effect of Incus Removal on Middle Ear Acoustic Sensor for a Fully Implantable Cochlear Prosthesis," *the 28th Annual International Conference of the IEEE Engineering in Medicine and Biology Society*, August 2006, pp. 539-542.
- [7] T. B. Gabrielson, "Mechanical-thermal noise in micromachined acoustic and vibration sensors", *IEEE Transactions on Electron Devices*, vol. 40, pp. 903-909, May 1993.
- [8] M. Suster, J. Guo, N. Chaimanonart, W. H. Ko, and D. J. Young, "A High-Performance MEMS Capacitive Strain Sensing Microsystem," *IEEE Journal of Microelectromechanical Systems*, Vol. 15, Issue 5, pp. 1069-1077, 2006.